Available online at www.sciencedirect.com
ScienceDirect
Nuclear Instruments and Methods in Physics Research A 583 (2007) 64–70
NUCLEAR INSTRUMENTS & METHODS IN PHYSICS RESEARCH Section A
www.elsevier.com/locate/nima

CCE measurements and annealing studies on proton-irradiated p-type MCz silicon diodes

H. Hoedlmoser[a,*], M. Moll[a], M. Koehler[b], H. Nordlund[c]

[a]CERN, 1211 Geneva 23, Switzerland
[b]University Siegen, Germany
[c]Helsinki Institute of Physics, Finland

Available online 31 August 2007

Abstract

Magnetic Czochralski (MCz) silicon has recently been investigated for the development of radiation tolerant detectors for future high-luminosity HEP experiments. A study of p-type MCz Silicon diodes irradiated with 24 GeV/c protons up to a fluence of 10^{16} p cm^{-2} has been performed by means of Charge Collection Efficiency (CCE) measurements as well as standard CV/IV characterizations. The changes of CCE, full depletion voltage and leakage current as a function of fluence are reported. A subsequent annealing study of the irradiated detectors shows an increase in effective doping concentration and a decrease in the leakage current, whereas the CCE remains basically unchanged. Two different series of detectors have been compared differing in the implantation dose of p-spray isolation as well as effective doping concentration (N_{eff}) of the p-type bulk presumably due to a difference in thermal donor (TD) activation during processing. The series with the higher concentration of TDs shows a delayed reverse annealing of N_{eff} after irradiation.

PACS: 85.30.De; 29.40.Gx; 29.40.Wk

Keywords: RD50; P-Type; MCz; Silicon; Radiation hardness; CCE; Annealing

1. Introduction

Silicon detectors intended for use in future experiments at high luminosity colliders such as an upgraded LHC or the SLHC with design luminosities exceeding 10^{34} cm^{-2} s^{-1} demand the development of detectors which can perform in extremely harsh radiation levels. The radiation damage suffered by the silicon results in an increase in leakage current, a change of full depletion voltage and an increased trapping of the drifting holes and electrons created by traversing charged particles. These three effects reduce the Charge Collection Efficiency (CCE) and the signal-to-noise ratio (S/N) of the detector. The ROSE collaboration [1] proved that oxygen enriched silicon features an increased radiation hardness toward charged particle irradiation [2] compared to standard float zone (FZ) silicon, which is used in most of the current HEP detectors. Recent technological advances allow the production of high-resistivity (up to a few kΩcm) magnetic Czochralski (MCz) silicon [3] with a typical oxygen concentration of $2-5\times10^{17}$ cm^{-3}, which is intrinsic due to the growth process, compared to a few 10^{16} cm^{-3} in standard material. With such a high oxygen concentration, it is expected to offer increased radiation tolerance when compared to FZ and even diffusion oxygenated FZ (DOFZ) silicon, which was confirmed in previous studies [4–9]. In this work p-type MCz diodes have been irradiated up to fluences of 10^{16} p cm^{-2} 24 with GeV/c protons and subsequently characterized in CCE evaluations as well as by means of standard CV/IV measurements and annealing studies. The following section describes the investigated material and gives details about the irradiation. Section 3 introduces the CCE setup and outlines the measurement procedures. In Sections 4–6 detailed results are given for the behavior of CCE, leakage current and V_{dep} following the irradiation and during annealing studies. Finally, Section 7 points out differences in the reverse-annealing time constants of some of the

*Corresponding author. Tel.: +41 76 487 3465.
E-mail address: Herbert.Hoedlmoser@cern.ch (H. Hoedlmoser).

0168-9002/$ - see front matter © 2007 Elsevier B.V. All rights reserved.
doi:10.1016/j.nima.2007.08.201

diodes, which are believed to be related to variations in TD concentration in the silicon.

2. Investigated material

The material investigated in the course of this study was 300 μm thick ⟨100⟩ p-type MCz silicon produced by Okmetic/Finland. The oxygen concentration of the material has been measured on four different positions on a 3 mm thick wafer by IR spectroscopy and was found to be $(4.95 \pm 0.03) \times 10^{17}$ at cm^{-3}. The square multi-guard ring diodes (diode area 13.7 mm^2) originate from two wafers with different p-spray concentrations (wafer W066 with 3×10^{12} cm^{-2} and W182 with 5×10^{12} cm^{-2}). The wafers also contained microstrip detectors and were processed together by ITC-IRST/Italy [10,11]. Before irradiation the diodes exhibited an inhomogeneity of the depletion voltage both within the wafer and between the two wafers. The eight diodes from the wafer W066 had values from 8 to 17 V and the eight from W182 from 97 to 110 V. According to information from ITC-IRST, the inhomogeneity within each full wafer was much larger than the range of the 8 diodes from each wafer. Recent work [12] shows that the differences in effective doping concentration are related to an inhomogenous concentration of TDs. A possible explanation could be a temperature gradient during the microstrip processing.

2.1. Irradiation

The detectors were irradiated with 24 GeV/c protons at the CERN PS [13] with fluences up to 10^{16} p cm^{-2}. The fluence received was measured with an accuracy of ±7% through spectroscopy of aluminum foil placed with the detectors in the PS beam during irradiation [13]. In some figures below the 1 MeV equivalent neutron fluence Φ_{eq} is cited, which was calculated from the proton fluence using a hardness factor of 0.62 [14]. For each fluence, one diode from each of the two distinct detector series was irradiated. After the irradiations the detectors were annealed for 4 min at 80 °C. At all other times the detectors were stored at −24 °C to minimize further annealing.

3. Experimental setup and procedures

The CCE measurements were performed by means of a setup which was obtained from NIKHEF [15]. As shown in Fig. 1, electrons originating from a collimated ^{90}Sr source are used to create charge in the investigated diode and a scintillator–photomultiplier combination provides the trigger for the readout electronics (combination of Amptek A250 integrating amplifier and two A275 shaper hybrids). The key parameters of the electronics are a signal shaping time of 2.5 μs, a gain calibration factor of 245 e$^-$/mV and an electronic noise of 567 e$^-$ + 4.26 e$^-$/pF. The diode is mounted on a sample PCB with the detector frontside and guard ring contacted by means of wire bonds and can be biased up to ±1000 V. The trigger rate achieved with the 3.7 MBq ^{90}Sr source is 50–60 Hz for a 300 μm diode. The measurement temperature can be adjusted with an integrated peltier element and the whole setup can be flushed with nitrogen and operated inside a small freezer to achieve temperatures as low as −25 °C. The measurements are controlled by LabVIEW software which collects a predefined number of events for a series of bias voltages and stores the signal values in a data file. Subsequently a LabVIEW analysis program is used to create a histogram and fit a Landau distribution to the data. The electronic noise is taken into account through a separate pedestal measurement which is used to correct the data for the pedestal offset and to deconvolute the gaussian noise spectrum and the Landau distributed signal. The fraction of pedestal events during a normal measurement is usually in the order of 2%. Fig. 2 shows an example for such an analysis. Unless specified differently, the most probable value of the deconvoluted Landau distribution was used for the CCE(V) or CCE(ϕ, V) plots. Measurements of irradiated diodes were found to be rather sensitive to

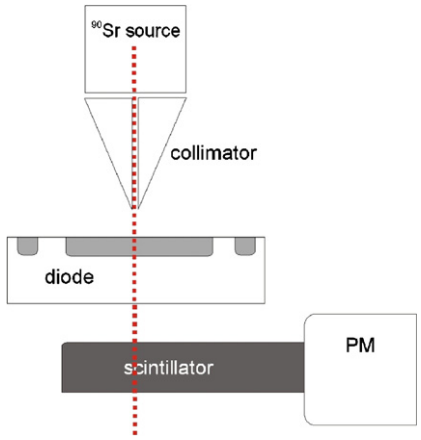

Fig. 1. Schematics of the CCE measurement system.

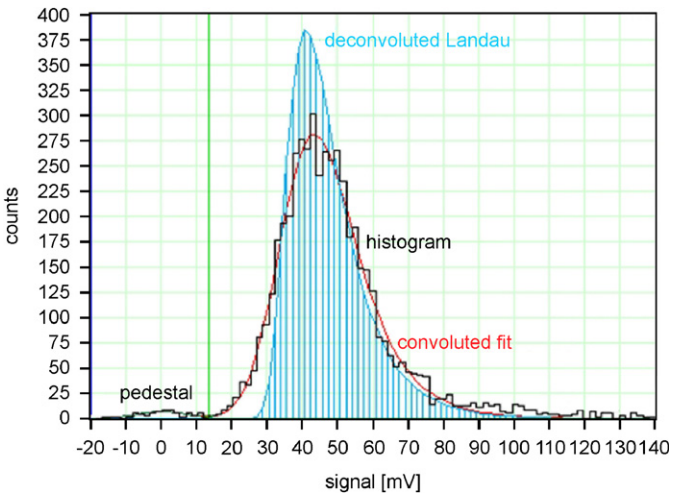

Fig. 2. Illustration of analysis of CCE measurements: the data were taken from a measurement at −10 °C of a detector irradiated with 3.5×10^{14} p cm^{-2} and annealed for 512 min at 80 °C.

temperature, possibly due to the rather long signal shaping time in combination with temperature dependent (de-) trapping effects. While for some of the highly irradiated diodes ($\phi \geqslant 10^{15}$ p/cm^2) the lowest possible temperature had to be used to be able to measure at all; for all other detectors it was attempted to keep the temperature at $-10\,^{\circ}$C to obtain reproducible results. In repeated measurements of an irradiated detector carried out during several days and involving repeated installation in the setup and cooldown to $-10\,^{\circ}$C, the most probable value of the Landau distribution could be reproduced within 3%.

IV and CV measurements were performed using a Keithley 2410 as a source meter, an Agilent 4263B LCR meter operating at 10 kHz in parallel mode and a Keithley 237 as a current meter. The DC supply voltage was decoupled from the small AC voltage of the LCR meter using capacitors. The rear p ohmic contact was connected to the bias voltage, the guard ring was connected to the ground and the signal line was connected to the front n^+ aluminium contact. The measurements were performed both at room temperature (RT) and at $-10\,^{\circ}$C. The leakage current measured at RT was corrected to $T_{\mathrm{ref}} = 20\,^{\circ}$C using

$$I(T_{\mathrm{ref}}) = \left(\frac{T_{\mathrm{ref}}}{T}\right)^2 \exp\left(\frac{-E_{\mathrm{g}}}{2k_{\mathrm{B}}}\left[\frac{1}{T_{\mathrm{ref}}} - \frac{1}{T}\right]\right) I(T) \qquad (1)$$

where E_{g} is the silicon band gap (1.12 eV) and k_{B} is the Boltzmann constant. The depletion voltage V_{dep} was obtained from the CV method by fitting straight lines to the log C versus log V plot and determining the intercept. Alternatively the V_{dep} was determined from the CCE measurements by fitting straight lines to the linear and constant sections of the $(\mathrm{CCE})^2$ versus V plots. The two methods are not in complete agreement; the determination of V_{dep} by the CCE method usually leads to a higher value than the CV method. For both methods V_{dep} was found to be dependent on the measurement temperature in the case of irradiated detectors. Fig. 9 in Section 6 provides an example for the difference between CCE and CV evaluation as well as for the influence of the temperature. It shows V_{dep} of an irradiated detector as a function of annealing time at 80 °C and contains curves obtained from the evaluation of CCE measurements at $-10\,^{\circ}$C as well as CV measurements at RT and $-10\,^{\circ}$C. The error bars given in the plots illustrate the inaccuracy of the line fits in the two evaluation methods, which is in the order of $\leqslant 5\%$. Other authors [16] report a better agreement of CCE and CV results, which could be attributed to their faster signal shaping (ns) in the CCE measurement.

4. Charge collection efficiency

Fig. 3 shows the CCE as a function of bias voltage of eight diodes of the W066 series, which have received different proton fluences in comparison with a non-irradiated detector, which shows a most probable charge

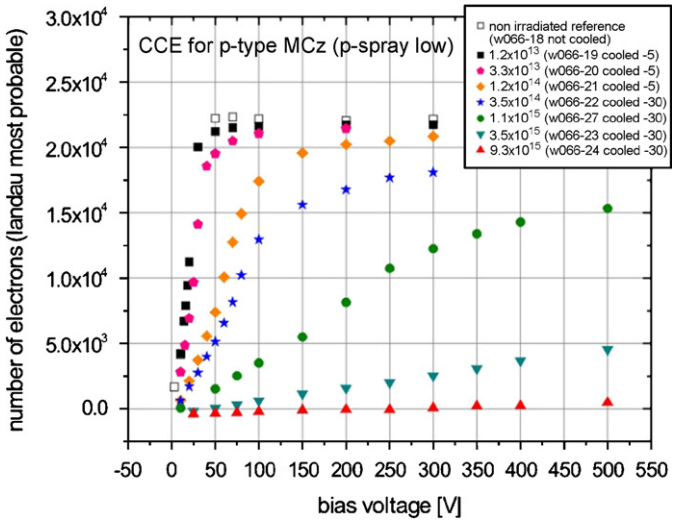

Fig. 3. CCE(V) curves for detectors of the W066 series irradiated with fluences up to 10^{16} p cm^{-2}.

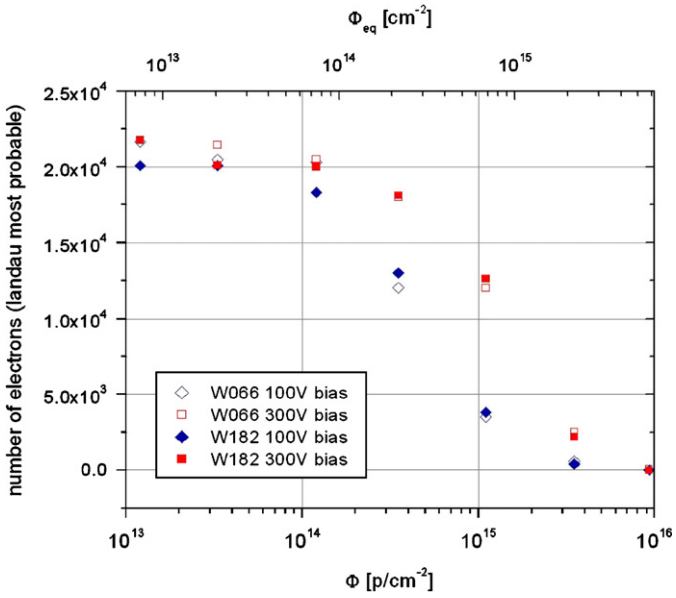

Fig. 4. CCE at 100 and 300 V bias as a function of received fluence for detectors of the W066 and W182 series.

signal of 22 000 electrons when fully depleted. Fig. 4 displays the CCE measured at 100 and 300 V bias as a function of the received proton fluence for both the detector series. The two series exhibit a similar behavior, with a CCE that is rapidly decreasing for fluences $\geqslant 10^{14}$ p cm^{-2} going to zero at 10^{16} p cm^{-2}.

In the annealing studies the CCE remained unchanged. The CCE(V) curves shown in Fig. 5 only reflect the change in depletion voltage described in Section 6, the maximum of the charge signal does not change. This behavior was confirmed in the annealing of diodes irradiated up to fluences of 10^{15} p cm^{-2} from both the detector series.

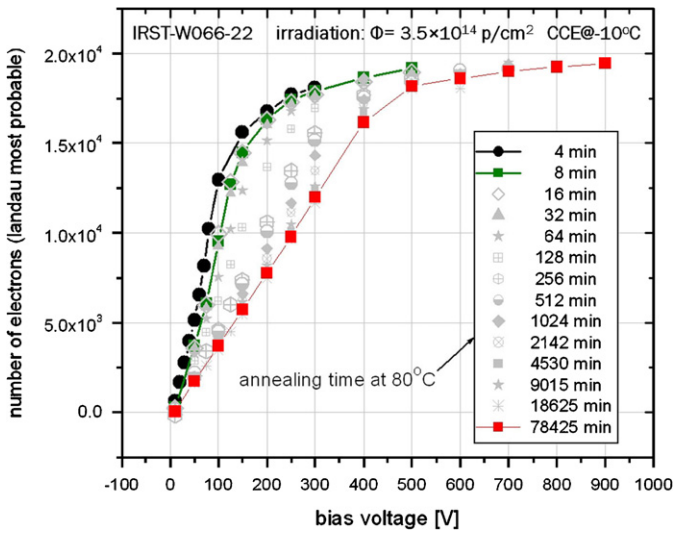

Fig. 5. CCE(V) curves at different stages of annealing at 80 °C. The curves reflect the change in depletion voltage, while the maximum charge signal remains unchanged.

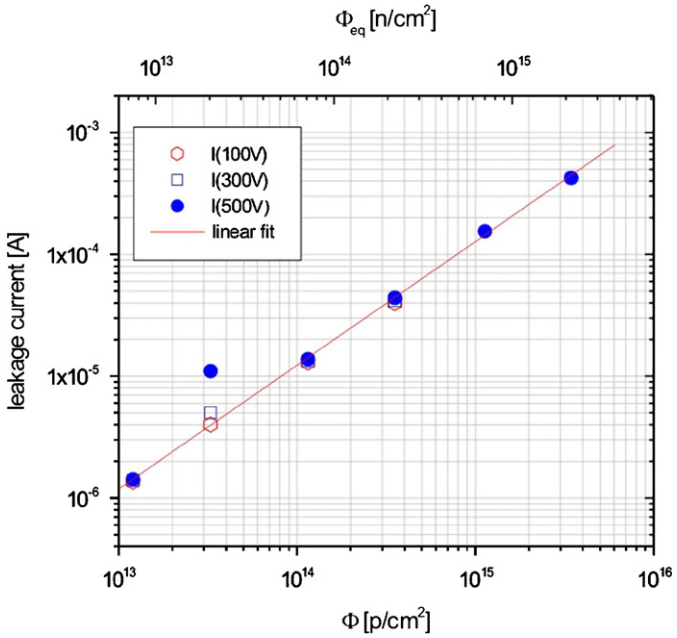

Fig. 6. Leakage current as a function of received fluence. Measurements performed at RT after a 4 min annealing step at 80 °C.

5. Leakage current

Before irradiation the leakage current of the fully depleted diodes was in or below the nA range. After irradiation the change in leakage current ΔI was measured as a function of fluence to determine the current related damage rate α which is defined by

$$\Delta I = \alpha \cdot \Phi_{\mathrm{eq}} \cdot V \tag{2}$$

with the detector volume V. Fig. 6 shows the leakage current as a function of received fluence. From the line-fit $\alpha = 4.9 \times 10^{-17}\,\mathrm{A\,cm^{-1}}$ was obtained.

In the subsequent annealing study, which was carried out at 80 °C, the annealing of α was investigated. The current measurements performed at RTs in the range of 21–30 °C had to be corrected according to Eq. (1) to allow a comparison with a parametrization of $\alpha(t)$ taken from [17]

$$\alpha(t) = \alpha_I \exp(-t/\tau_I) + \alpha_0 + \beta \ln(t/t_0) \tag{3}$$

with $\alpha_I = 1.13 \times 10^{-17}\,\mathrm{A\,cm^{-1}}$, $\tau_I = 9\,\mathrm{min}$, $\alpha_0 = 4.23 \times 10^{-17}\,\mathrm{A\,cm^{-1}}$, $\beta = 2.83 \times 10^{-18}\,\mathrm{A\,cm^{-1}}$ and $t_0 = 1\,\mathrm{min}$ for annealing at 80 °C. These parameters were determined from measurements on different types of silicon other than MCz. Fig. 7 shows $\alpha(t)$ obtained from the measurements of three different diodes irradiated with two different fluences in comparison to Eq. (3) and to the α-value taken from the fit in Fig. 6. Given the rather large corrections of the measured current values due to the large variations in measurement temperature, the agreement of measurement and parametrization is satisfying, and it can be concluded that the p-type MCz behaves similar to other types of silicon.

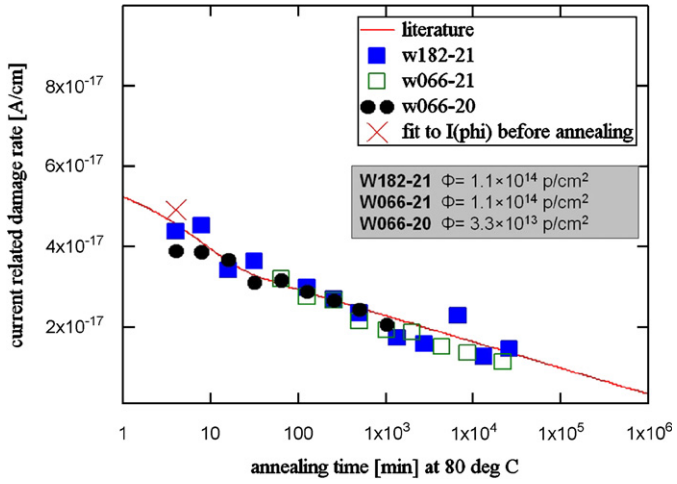

Fig. 7. Current related damage rate α as a function of annealing time at 80 °C. Current measurements were performed at RT and corrected to 20 °C according to Eq. (1). The plotted line corresponds to Eq. (3) and the red × is the α-value taken from Fig. 6.

6. Full depletion voltage

Fig. 8 shows V_{dep} of the two series of diodes as a function of received proton fluence as obtained from CV measurements at RT. For the W182-series, which is presumed to have a lower TD concentration, V_{dep} is decreasing down to 50 V at a fluence of $10^{14}\,\mathrm{p\,cm^{-2}}$, while V_{dep} of the W066 series remains constant at the lower level. For higher fluences V_{dep} increases for both series up to ~280 V at $10^{15}\,\mathrm{p\,cm^{-2}}$.

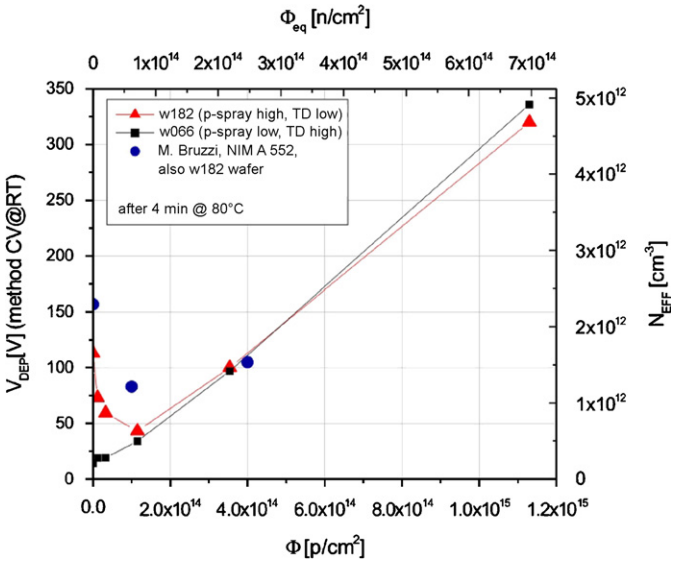

Fig. 8. Change in effective doping concentration of the two detector series as a function of received fluence.

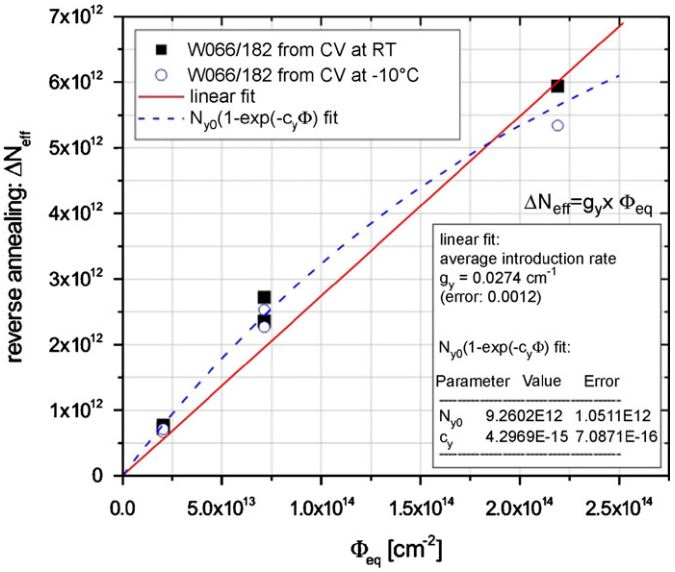

Fig. 10. Change in effective doping concentration during reverse annealing as a function of fluence. For this evaluation only the evaluation of V_{dep} by the CV method has been used.

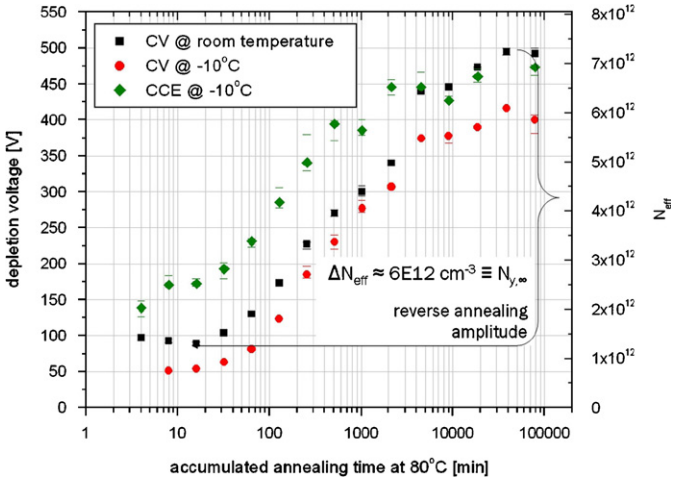

Fig. 9. Reverse annealing of a diode irradiated with $3.5 \times 10^{14}\,\mathrm{p\,cm^{-2}}$. V_{dep} was evaluated from both CCE and CV measurements at different temperatures. The error bars correspond to the uncertainty of the line fits in the log C(log V) and CCE^2(V) plots.

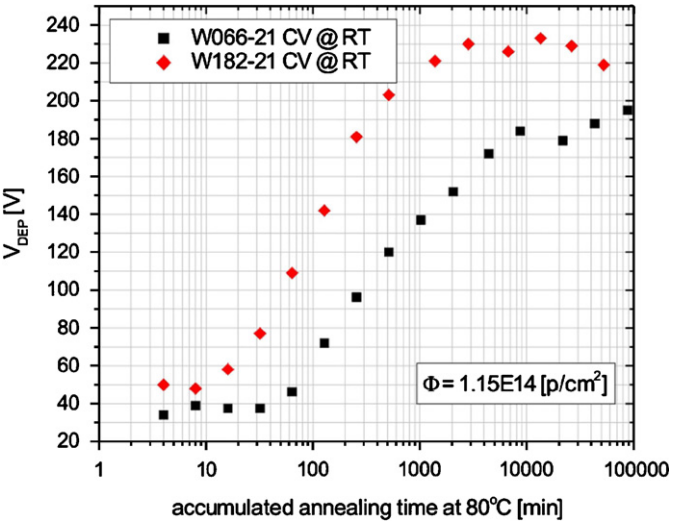

Fig. 11. Comparison of the reverse-annealing behavior of the two diodes W066-21 and W182-21, which have both received a fluence of $1.15 \times 10^{14}\,\mathrm{p\,cm^{-2}}$. V_{dep} is evaluated from CV measurements at RT.

Annealing studies were carried out for detectors of both series up to received fluences of $10^{15}\,\mathrm{p\,cm^{-2}}$. Fig. 9 shows the change in N_{eff} during the reverse annealing of a detector irradiated with $3.5 \times 10^{14}\,\mathrm{p\,cm^{-2}}$, i.e. the reverse-annealing amplitude $N_y(t)$. In Fig. 10 the final value of the reverse-annealing amplitude, $N_{y,\infty}$, is plotted against the received fluence. From the line fit to the data points, a generation rate $g_y = 2.74 \times 10^{-2}\,\mathrm{cm^{-1}}$ was determined which is in agreement with previously published data about Cz silicon [17]. As these results cover only three different proton fluences, it is impossible to determine if $N_{y,\infty}$ saturates for higher fluences. However, signs for a saturation are visible as indicated by the $N_{y,0}(1-\exp(-c\cdot\phi))$ fit, where $N_{y,0}$ is the value $N_{y,\infty}$ approaches for the highest fluences.

7. Differences in annealing of V_{dep} due to thermal donors

In the annealing studies it was found that all the investigated diodes from the W066 series, which is presumed to have a higher TD concentration, showed a delayed reverse annealing in comparison with the W182 series. This behavior is illustrated in Fig. 11 in which V_{dep} is plotted as a function of annealing for one diode from each series irradiated with $1.15 \times 10^{14}\,\mathrm{p\,cm^{-2}}$. This effect has been confirmed in independent evaluations of the depletion voltage by the CCE method and the CV method. Furthermore it could be reproduced in annealing studies of

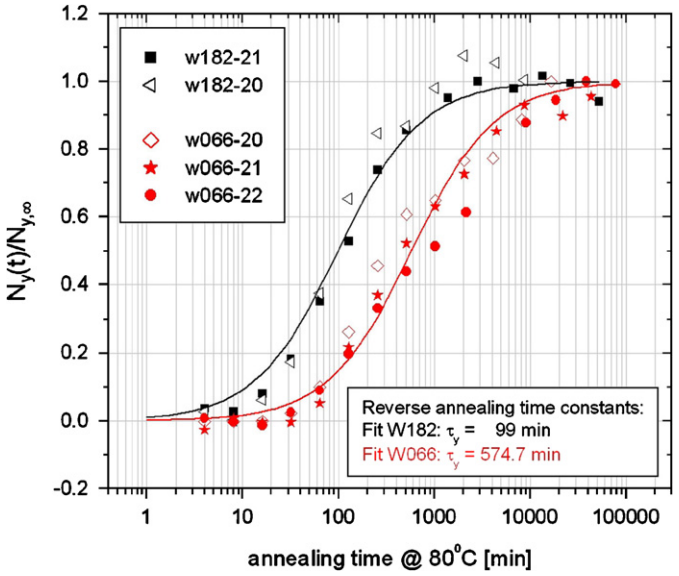

Fig. 12. $N_y(t)/N_{y,\infty}$ for five detectors from both types and fits of Eq. (4) to the data.

detectors irradiated with four different fluences. In each case the increase of N_{eff} started earlier for the diodes from the W182 series. It was attempted to fit the annealing data obtained for the two detector series with the following parametrization taken from [17]

$$N_y(t) = N_{y,\infty}\left(1 - \frac{1}{1 + t/\tau_y}\right). \quad (4)$$

$N_{y,\infty}$ is the maximum reverse-annealing amplitude as shown in Fig. 9 and τ_y is the reverse-annealing time constant. Fig. 12 contains the plots of $N_y(t)/N_{y,\infty}$ as well as the fits of Eq. (4) to the data from the two series. The values of the annealing time constant τ_y derived from these fits are 99 min for the W182 diodes and 575 min for the W066 diodes. This result emphasizes the distinct behavior of the two diode types, which is assumed to be a consequence of the higher TD concentration in the W066 diodes.

8. Summary and outlook

In this work two series of 300 μm p-type MCz diodes have been irradiated up to fluences of 10^{16} p cm^{-2} 24 GeV/c protons and subsequently characterized in CCE and CV/IV measurements and annealing studies. The measurements with the newly commissioned CCE setup showed a rapid decrease of the CCE(300 V) starting at a received fluence of 10^{14} p cm^{-2}. At 10^{15} p cm^{-2} the CCE(300 V) is at 55% and it drops to zero at 10^{16} p cm^{-2}. During annealing studies the maximum CCE remains constant. The CCE and V_{dep} derived from the CCE(V) curves were found to be temperature dependent. The increase in leakage current due to irradiation and the annealing behavior of the current related damage rate were found to be in agreement with previously measured data for other types of Si. The two series of irradiated diodes were differing not only in the p-spray concentration at the surface, but also exhibited different depletion voltages before irradiation, which can be assumed to be due to a different concentration of TDs. From the point of view of CCE and leakage current no major differences were found between the two series. The evolvement of V_{dep} due to irradiation and subsequent annealing, however, was different. For the series with the lower TD concentration and consequently higher initial value of V_{dep}, the depletion voltage is decreasing with the fluence up to of 10^{14} p cm^{-2}, while V_{dep} of the series with the higher TD concentration (lower initial depletion voltage) remains constant at the lower level. Only for higher fluences V_{dep} increases for both series up to ~280 V at 10^{15} p cm^{-2}. The reverse annealing of V_{dep} exhibited an even more significant difference between the two series. All the detectors with higher TD concentrations showed a delayed reverse annealing with time constants at least a factor of 5 higher than for the second series. As it is rather unlikely that the observed differences are related to the difference in p-spray implantation dose, it seems that a high TD concentration in p-type MCz not only allows to adjust V_{dep} to a lower initial level but also leads to a higher stability for the low fluences and to a delayed reverse annealing.

It is currently being attempted to irradiate and characterize other types of Si for comparison with the results obtained for the p-type MCz. Regarding the possible influence of TDs on the performance of the p-type MCz a new series of tests is foreseen: as the variation of V_{dep} between the two detector series was a rather accidental feature, it is planned to heat-treat a series of p-type MCz diodes specifically to engineer a range of initial values for V_{dep} as described in Ref. [18] and then repeat the above-described tests in order to reproduce the results in a systematic way.

Acknowledgments

We would like to thank F. Hartjes, who was an invaluable help in the commissioning of the NIKHEF CCE system. Furthermore we would like to thank M. Glaser and his team for the irradiations at the PS irradiation facility, B. Surma for the IR spectroscopy and I. McGill and his team at the bondlab of the CERN silicon facility for contacting the diodes for our measurements.

References

[1] The ROSE Collaboration (R&D On Silicon for future Experiments), CERN-RD48 Collaboration, ⟨http://rd48.web.cern.ch/RD48/⟩.
[2] G. Lindstrom, et al., Nucl. Instr. and Meth. A 466 (2001) 308.
[3] V. Savolainen, et al., J. Cryst. Growth 243 (2003) 2.
[4] A.G. Bates, et al., LHCb-2004-052 VELO, 2004.
[5] J.P. Palacios, et al., Nucl. Instr. and Meth. A 535 (2004) 428.
[6] J. Harkonen, et al., Nucl. Instr. and Meth. A 541 (2005) 202.
[7] P. Luukka, et al., Nucl. Instr. and Meth. A 530 (2004) 117.
[8] Z. Li, et al., IEEE Trans. Nucl. Sci. NS-51 (4) (2004).

[9] A.G. Bates, et al., Nucl. Instr. and Meth. A 555 (2005) 113124.
[10] A. Pozza at the 2nd Trento Workshop, 2006 ⟨http://tredi.itc.it/program/talks/p-type/pozza.ppt⟩.
[11] M. Bruzzi, et al., Nucl. Instr. and Meth. A 552 (2005) 20.
[12] D. Menichelli, Workshop on defect analysis in radiation damaged silicon detectors, Hamburg-DESY, August-2006. ⟨http://wwwiexp.desy.de/seminare/defect.analysis.workshop.august.2006/menichelli_hamburg06.ppt⟩.
[13] M. Glaser, et al., Nucl. Instr. and Meth. A 426 (1999) 72.
[14] M. Moll, et al., Nucl. Instr. and Meth. B 186 (2002) 100.
[15] Description and manual of the NIKHEF CCE setup: ⟨http://www.nikhef.nl/~i56/Manual.pdf⟩.
[16] G. Kramberger at the 8th RD50 Workshop in Prag 2006. ⟨http://rd50.web.cern.ch/rd50/8th-workshop/default.htm⟩.
[17] M. Moll, Radiation damage in silicon particle detectors—microscopic defects and macroscopic properties, Ph.D. Thesis, DESY-THESIS-1999-040, University of Hamburg, December 1999.
[18] M. Bruzzi, et al., J. Appl. Phys. 99 (2006) 093706.